

# Signatures of Nucleon Disappearance in Large Underground Detectors

Yuri Kamyshev\*

Department of Physics, University of Tennessee, Knoxville, TN 37996

Edwin Kolbe†

Physics Division, Oak Ridge National Laboratory, Oak Ridge, TN 37831

For neutrons bound inside nuclei, baryon instability can manifest itself as a decay into undetectable particles (e.g.,  $n \rightarrow \nu\nu\bar{\nu}$ ), i.e., as a disappearance of a neutron from its nuclear state. If electric charge is conserved, a similar disappearance is impossible for a proton. The existing experimental lifetime limit for neutron disappearance is 4-7 orders of magnitude lower than the lifetime limits with detectable nucleon decay products in the final state [1]. In this paper we calculated the spectrum of nuclear de-excitations that would result from the disappearance of a neutron or two neutrons from  $^{12}\text{C}$ . We found that some de-excitation modes have signatures that are advantageous for detection in the modern high-mass, low-background, and low-threshold underground detectors, where neutron disappearance would result in a characteristic sequence of time- and space-correlated events. Thus, in the KamLAND detector [2], a time-correlated triple coincidence of a prompt signal, a captured neutron, and a  $\beta^+$  decay of the residual nucleus, all originating from the same point in the detector, will be a unique signal of neutron disappearance allowing searches for baryon instability with sensitivity 3-4 orders of magnitude beyond the present experimental limits.

PACS number(s): 24.80.+y, 13.30.Ce, 14.20.-c, 24.10.Pa

## I. INTRODUCTION

Baryon asymmetry of the universe [3] and the idea of unification of particle and forces [4, 5] are the two global concepts that motivated the nucleon decay experimental searches [6] for more than two decades. The particular modes of nucleon decay are not known a priori, although some are preferred by theoretical models [4, 5, 7, 8]. The results from several generations of nucleon decay search experiments [1], including the most spectacular recent Super-Kamiokande results [9], have set stringent limits on many exclusive nucleon decay modes. For example, the lifetime limit for the decay mode  $p \rightarrow e^+ + \pi^0$ , established by the Super-K Collaboration, reaches  $\tau_p \geq 5 \cdot 10^{33}$  years [10]. However, the mode-independent nucleon lifetime limit [1] is established experimentally only at the level of  $\geq 1.6 \cdot 10^{25}$  years [11], which is more than 8 orders of magnitude poorer than the previous limit. That indicates that experimental searches for certain decay modes need to be extended.

The Particle Data Group identifies 75 possible modes of nucleon decay (baryon instability) [1] that respect the conservation laws of electric charge, energy-momentum, and angular momentum. The lifetime limits for most of these modes lie above  $10^{30}$  years, but there are a few significant exceptions. These are the modes corresponding to the decay of one neutron or two neutrons into neutrinos:  $n \rightarrow 3\nu$ ,  $n \rightarrow 5\nu$ , and  $nn \rightarrow 2\nu$ . Lifetime

limits for these modes are several orders of magnitude lower [1]. Generally speaking, these modes can be interpreted as disappearance of one or two neutrons from their intra-nucleus state into any undetectable particles. Following the spirit of the paper of Evans and Steinberg [11] and using the assumptions of the conservation laws mentioned above, one could think that the present “mode-independent” nucleon decay limit [1] is determined by these neutron disappearance modes. We believe that experimental searches for these modes and the improvement of mode-independent nucleon lifetime limit are as fundamentally important as searches for particular exclusive nucleon decay modes with super-giant detectors.

Moreover, decays like  $N \rightarrow \text{lepton} + \text{lepton} + \text{antilepton}$  arise in certain unification schemes [4, 12] as a result of  $(B - L)$  non-conserving interactions that might be more natural for the explanation of baryon asymmetry of universe than  $(B - L)$ -conserving transitions. The question of whether  $(B - L)$  is violated in nature and at what energy scale can be answered only by experiments [13]. Nucleon decay into five and more leptons was theoretically considered in [4]; dinucleon decay into two leptons in [14].

In this paper we demonstrate that the disappearance of a neutron (or two neutrons) from its intra-nucleus state creates subsequent nuclear de-excitations that, for a few particular de-excitation modes, would lead to a unique experimental signature: *a chain of time- and space-correlated events*. Such a signature can be observed in the modern large-mass, low-background, and low-threshold detectors, e.g., in KamLAND [2]. We estimate that the sensitivity of a search for such events in the KamLAND detector will result in improvement of

---

\*Electronic address: kamyshev@utk.edu

†Electronic address: kolbe@quasar.physik.unibas.ch

one-neutron and two-neutron disappearance limits by 3-4 orders of magnitude beyond the existing lifetime limits.

The idea that nucleon decay in the nucleus can be studied by measuring particles and/or  $\gamma$  rays accompanied by de-excitation of the nucleon hole was, to our knowledge, first considered by Y. Totsuka [15] and H. Ejiri [16] and used by the Kamiokande Collaboration [17] as discussed below. Also, recently the DAMA Collaboration [18] has searched in 6.5 kg of a liquid  $^{129}\text{Xe}$  scintillator detector operating in Gran Sasso National Laboratory for the decay products of the residual radioactive daughter nuclei left after the disappearance of one or two nucleons from a  $^{129}\text{Xe}$  nucleus and set new limits for two-nucleon disappearance.

In section II of this paper, we discuss the existing experimental limits for  $n \rightarrow 3\nu$ ,  $nn \rightarrow 2\nu$ , and, in general, for disappearance of one or two neutrons. Our calculations for de-excitation branching ratios in intra-nucleus disappearance of one neutron from  $^{12}\text{C}$  are discussed in section III; for comparison, in section IV, we also calculated the disappearance of a neutron from an  $^{16}\text{O}$  nucleus; section V deals with the calculations of de-excitation modes following the two-neutron disappearance from  $^{12}\text{C}$ . The possible observation of some particular de-excitation modes followed by the radioactive decay of daughter nuclei in the KamLAND detector, as well as the possible sources of background, are discussed in section VI. Our conclusions are presented in section VII.

## II. EXISTING LIMITS FOR NEUTRON DISAPPEARANCE

Experimental limits have been set for  $n \rightarrow 3\nu$  decay in underground experiments [19, 20] assuming that the whole Earth is the source of decaying neutrons. The underground detectors in this case measure the specific energy spectrum above the background level of atmospheric neutrino signals, resulting from decay-neutrinos interactions with the material of the detector. The best limit set from the analysis of the muon events induced by charge-current  $\nu_\mu$  interactions in the detector [19] was  $\tau(n \rightarrow 3\nu_\mu) > 5 \cdot 10^{26}$  years. The best limit from  $\nu_e$  interactions was set in [20] as  $\tau(n \rightarrow 3\nu_e) \geq 3 \cdot 10^{25}$  years. Due to the detection method, these limits are only valid for the specific decay of a neutron into particular types of neutrinos and cannot generally be applied to the neutron disappearance.

A very inspirational approach has been used by the Kamiokande Collaboration [17] who set the limit for  $n \rightarrow \nu\nu\bar{\nu}$  decay of  $\tau \geq 4.9 \cdot 10^{26}$  years, independent of the type of neutrinos emitted in the neutron decay. By virtue of the experimental method, this limit is also relevant for intra-nucleus neutron disappearance. The method is based on the detection of  $\gamma$ -rays, which could be residual de-excitation products of a highly excited  $^{15}\text{O}$  nucleus left after the disappearance of a neutron from  $^{16}\text{O}$  in the

low-background energy range between 19 and 50 MeV. Because of the similarity to our approach, we are discussing this method below in more detail. In this regard we also refer to the paper by H. Ejiri [16].

When a neutron disappears from the oxygen nucleus, the residual  $^{15}\text{O}$  is often left in an excited state. In the nuclear shell model the excitation level is determined by the level that a neutron has inside the  $^{16}\text{O}$  and by the width of this energy level (spreading width). In the  $^{16}\text{O}$  nucleus, two neutrons occupy the lowest  $s_{1/2}$  level, 4 neutrons fill the next  $p_{3/2}$  shell, and the remaining 2 neutrons populate the highest  $p_{1/2}$  state. The disappearance of a neutron from the  $p_{1/2}$  state would result in a minimal excitation where the residual  $^{15}\text{O}$  with high probability will be left in the ground state and the difference of the binding energy will be taken care of by undetected neutron decay products. The disappearance of a neutron from a lower  $p_{3/2}$  state will create a hole that will result in a restructuring of the residual nucleus with possible emission of  $\gamma$  radiation. Thus, it was estimated in [17] that de-excitation of the  $p_{3/2}$  neutron hole with a probability of  $\sim 44\%$  will produce 6.18 MeV  $\gamma$ -rays. The remaining part the  $^{15}\text{O}$  nucleus will again be left in the ground state. When a disappearing neutron produces a hole in the  $s_{1/2}$  shell, the excitation energy is large enough to exceed the separation energy for protons and neutrons in  $^{15}\text{O}$ . In this case de-excitation proceeds mainly by emission of a proton, neutron,  $\alpha$ , and, to a smaller extent, by emission of  $\gamma$ s. Since the Kamiokande water-Cherenkov detector was not sensitive to low-energy protons, neutrons,  $\alpha$ s, and had a threshold for  $\gamma$  and electron detection of 7.5 MeV, the authors of paper [17] concentrated only on the probability of de-excitation of the  $s_{1/2}$ -state hole via emission of  $\gamma$ s within an energy range of 19-50 MeV, where the experimental background was very small. This resulted in a rather small de-excitation branching ratio (Br) estimated in [17] as  $(0.27 - 1.04) \cdot 10^{-4}$ . Due to this small branching ratio, the measured  $\tau/Br = 1.8 \cdot 10^{31}$  years in the Kamiokande detector has resulted in  $\tau_{n \rightarrow 3\nu}$  disappearance limit of only  $\geq 5 \cdot 10^{26}$  years.

For completeness, we need to mention that the Particle Data Group listings [1] also include the  $n \rightarrow 3\nu$  and  $n \rightarrow 5\nu$  lifetime limits of the J.-F. Glicenstein analysis [21]  $\tau(n \rightarrow 3\nu_X) \geq 2.3 \cdot 10^{27}$  years and  $\tau(n \rightarrow 5\nu_X) \geq 1.7 \cdot 10^{27}$  years, based on the Kamiokande experimental data and on the idea that the disappearance of the neutron's magnetic moment should produce radiation.

Existing lifetime experimental limits for  $nn \rightarrow 2\nu$  are even less stringent. The following two limits were determined by the Fréjus Collaboration [20]:  $\tau(nn \rightarrow 2\nu_e) \geq 1.2 \cdot 10^{25}$  years and  $\tau(nn \rightarrow 2\nu_\mu) \geq 6.0 \cdot 10^{24}$  years. These limits assume two-neutron decays into neutrinos and antineutrinos of  $e$  and  $\mu$  flavors rather than the more general intra-nucleus disappearance of two neutrons. Recently the DAMA Collaboration [18], looking for the de-excitation products of the residual radioactive daughter nuclei left after the two-neutron disappearance from a  $^{129}\text{Xe}$ , has set the lower limit for  $nn \rightarrow 2\nu$  (more gen-

erally for two-neutron disappearance) as  $\tau(nn \rightarrow 2\nu) \geq 1.2 \cdot 10^{25}$  years.

### III. NEUTRON DISAPPEARANCE FROM $^{12}\text{C}$

Large liquid scintillator detectors like KamLAND [2] and Borexino [22] contain  $^{12}\text{C}$  as a major component of the detector material. In the simple nuclear shell-model picture the  $^{12}\text{C}$  ground state is described as a closed-shell nucleus i.e., for both protons and neutrons the lowest-lying  $s_{1/2}$  and  $p_{3/2}$  shells are completely filled, while all higher (sub)shells are empty. This occupation of the nuclear energy levels by neutrons is sketched in Figure 1. Thus, most of the neutrons available in liquid scintillator detectors for the baryon instability search are the neutrons occupying  $s_{1/2}$  and  $p_{3/2}$  energy levels in  $^{12}\text{C}$ .

#### A. Disappearance from the $p_{3/2}$ shell

If, in the simple shell-model picture, a neutron disappears from the  $p_{3/2}$  shell in  $^{12}\text{C}$ , the residual  $^{11}\text{C}$  nucleus is always left in the ground state. However, in more sophisticated shell-model calculations, it has been shown that the simple closed-shell picture of the  $^{12}\text{C}$  ground state has to be remedied. Due to correlations, especially pairing effects, the  $p_{1/2}$  shell is also partially filled with protons and neutrons from the  $p_{3/2}$  level lying just 4.44 MeV below (Fig.1). Various shell-model calculations [23] give partial occupation numbers of the  $p_{1/2}$  shell for both neutrons and protons in the range 0.75–0.8, corresponding to an average filling of the  $p_{3/2}$  shell between 3.2 and 3.25. If we interpret the partial occupations by saying that approximately 60 percent of the time the  $p_{3/2}$  shell is completely filled, while roughly 40 percent of the time two neutrons (the same for a proton pair) are in the  $p_{1/2}$  shell, then there is a finite probability that a

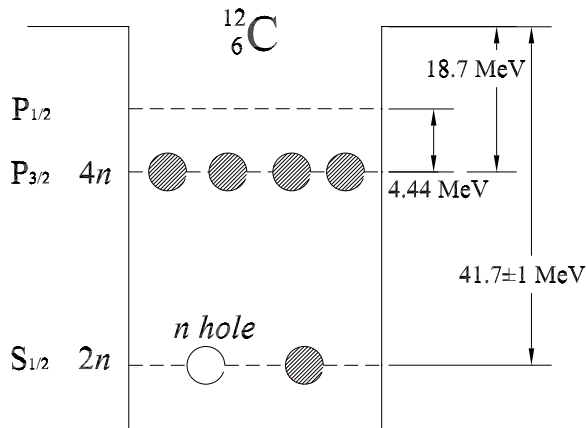


FIG. 1: Occupation of energy levels by neutrons for the  $^{12}\text{C}$  ground state in a simple shell model picture. One neutron is shown as disappeared from  $s_{1/2}$  level.

neutron disappearing from the  $p_{3/2}$  state will leave the residual  $^{11}\text{C}$  nucleus in an excited state with spin and parity  $J^\pi = 1/2^-$ . There is only one state in  $^{11}\text{C}$  with  $J^\pi = 1/2^-$  below 10 MeV [24], which is the first excited state at 2.0 MeV. Therefore, we assume that this is the only possible final state when a  $p_{3/2}$  neutron disappears, while at the same time a pair of neutrons is in the  $p_{1/2}$  shell, i.e., we assume the corresponding spectroscopic factor to be 1. Then the probability per P-shell neutron for this event is given by the product of 40 percent and 1/2, that is 20 percent, with an adopted error of  $\pm 5\%$ . The first excited state in  $^{11}\text{C}$  will promptly de-excite by emission of a  $\gamma$  with an energy of 2.0 MeV, and the ground state of  $^{11}\text{C}$  will subsequently undergo a  $\beta^+$  transition (the half-lifetime of  $^{11}\text{C}$  is 20.4 min and  $Q_{EC} = 1.98$  MeV).

Thus, the disappearance of a neutron from the  $p_{3/2}$  state will result, with a branching of  $20 \pm 5\%$  per each of four P-shell neutrons, in two time-correlated events: emission of monoenergetic 2.0 MeV  $\gamma$  and  $\beta^+$  emission with detectable energy in the range 1.02–1.98 MeV.

#### B. Disappearance from the $s_{1/2}$ shell

A more complicated and rich picture emerges if a neutron disappears from the  $s_{1/2}$  state in  $^{12}\text{C}$ . Excitation energy of the residual  $^{11}\text{C}^*$  in this case is very high; it exceeds the separation energy for proton, neutron, and  $\alpha$  particles in  $^{11}\text{C}$ , making them the primary emission products of the highly excited nucleus. Qualitatively, emission of a proton should be more frequent than emission of a neutron, since  $^{11}\text{C}$  is a proton-rich nucleus. Primary emission might not be sufficient for removing all the excitation energy and therefore might be followed by secondary de-excitation. Nuclear model calculations are needed in order to estimate these particular de-excitation branching ratios.

The residual  $^{11}\text{C}$  nucleus is left in a highly excited state with (assuming conservation of angular momentum and parity) total spin and parity  $J^\pi = \frac{1}{2}^+$ . The excitation energy  $E^*$  of this state can be calculated by the difference between the binding energy of the  $s_{1/2}$  neutron level in  $^{12}\text{C}$  and the neutron separation energy of  $^{12}\text{C}$ . While the latter is well known to be  $S_n = 18.72$  MeV, no precise experimental or theoretical values exist for the binding energy of the  $s_{1/2}$  neutron level. In the case of the  $s_{1/2}$  proton level in  $^{12}\text{C}$  the binding energy and the width have been measured in several electron scattering experiments  $^{12}\text{C}(e, e'p)$  [25] and were determined to be  $E_{1S}^p = 39 \pm 1$  MeV and  $\Gamma_{1S}^p = 12 \pm 3$  MeV, respectively. Correcting  $E_{1S}^p$  for the Coulomb shift of  $\approx 2.7$  MeV for protons in  $^{12}\text{C}$  gives us  $E_{1S}^n = 41.7 \pm 1$  MeV for the binding energy of the  $s_{1/2}$  neutron level in  $^{12}\text{C}$  and, subtracting the neutron separation energy, we get the value  $E^* = 23 \pm 1$  MeV for the excitation energy in  $^{11}\text{C}$ . Determination of width of the excited state caused by the dis-

appearance of  $s_{1/2}$  nucleon is not that straightforward. In terms of nuclear correlations that are responsible for the width of the excited state, the disappearance of nucleon a priori is not the same process as the knocking-out of a nucleon, since in the latter case a strongly-interacting particle remains present in the final state inside the nuclear matter. Different approaches are possible here. Theoretical estimates for the spreading width of the  $s_{1/2}$  hole in infinite nuclear matter [26] gives a value of  $\sim 6$  MeV. As another extreme one can use the spreading width of  $s_{1/2}$  state as determined in proton knock-out experiments [25]. We adopt what we think is a reasonable compromise here and assumed that the excited level at  $E^* = 23 \pm 1$  MeV in  $^{11}\text{C}$  has a Lorentzian width of  $\Gamma = 7$  MeV. At the end of the section we will show that our main results do not sensitively depend on the values adopted for  $E^*$  and  $\Gamma$  in the whole range of variations mentioned above.

In order to determine the de-excitation modes of the excited  $^{11}\text{C}$  nucleus, i.e., the branching ratios in the various particle emission channels and the energy spectra of the emitted particles, we used the statistical model of compound nuclear reactions (Hauser-Feshbach) [27]. Within this model the branching ratio for the decay  $A^*(c)A_c$  of an excited state of a nucleus  $A$  with energy  $E^*$  and spin and parity  $J^\pi$  to a final nucleus  $A_c$  by emission of a particle  $c$  is given by the ratio of the transmission coefficients:

$$Br_c(E^*, J^\pi) = \frac{T_c(E^*, J^\pi)}{T_{tot}(E^*, J^\pi)} \quad (1)$$

Here  $T_{tot}$  is simply the sum of the transmission coefficients of all decay channels open at  $E^*$ :

$$T_{tot}(E^*, J^\pi) = \sum_c T_c(E^*, J^\pi) \quad (2)$$

which guarantees that the sum of the branching ratios is normalized to one. Each of the transmission coefficients  $T_c$  is obtained by adding the contributions from all allowed final states in the residual nucleus:

$$T_c(E^*, J^\pi) = \sum_{\mu=0}^{N_c} T_c^\mu(E^*, J^\pi, E_c^\mu, J_c^\mu, \pi_c^\mu) + \int_{\bar{E}_c^{N_c}}^{E^* - S_c} \sum_{J_c, \pi_c} T_c(E^*, J^\pi, E_c, J_c, \pi_c) \rho(E_c, J_c, \pi_c) dE_c \quad (3)$$

In this sum the decays to the ground state ( $\mu = 0$ ) and all experimentally known excited levels ( $\mu = 1, 2, \dots, N_c$ ) in the daughter-nucleus are explicitly taken into account. For excitation energies higher than the energy  $E_c^N$  of the last known level the sum is changed to an integration over the level density  $\rho$  up to the highest energetically allowed state at energy  $E^* - S_c$ , where  $S_c$  is the channel separation energy for the ejected particle  $c$ . It can be seen, that the important ingredients of statistical model calculations are the particle and  $\gamma$ -transmission coefficients

$T$  and the level density of the excited states. Therefore, the quality of the calculated results within the statistical model is determined by the accuracy with which these components can be evaluated.

The branching ratios and particle energy spectra we present in the following have been calculated with the statistical model code SMOKER [28], which applies realistic optical potentials (reproducing nicely experimental data) to determine the transmission coefficients and a sophisticated description for the level density (by a combination of a constant temperature formula and a back-shifted Fermi gas). Starting from an excited state with well-defined energy, angular momentum, and parity, the SMOKER program calculates the branching ratios for transitions via photon, neutron, proton, and  $\alpha$  emission, which are the dominant de-excitation channels. Note that within SMOKER the transmission coefficients in Eq. (3) describing the transition from the excited state  $(E^*, J^\pi)$  to the state  $(E_c^\mu, J_c^\mu, \pi_c^\mu)$  in the daughter nucleus are correctly obtained by summing up the contributions from all quantum mechanically allowed partial waves:

$$T_c^\mu(E^*, J^\pi, E_c^\mu, J_c^\mu, \pi_c^\mu) = \sum_{l=|J-s|}^{J+s} \sum_{s=|J_c^\mu - j_c|}^{J_c^\mu + j_c} T_{c_l s}(E^* - S_c - E_c^\mu) \quad (4)$$

Here angular momentum  $\vec{l}$  and the channel spin  $\vec{s} = \vec{j}_c + \vec{J}_c^\mu$  couple to  $\vec{J} = \vec{l} + \vec{s}$ . For the physical quantities typically needed in statistical model calculations (e.g., nuclear masses, level density parameters), SMOKER takes the experimental values, if they exist. Otherwise, theoretical models are applied. This is illustrated in Figure 2, where the branching ratios for the decay of an excited state of  $^{11}\text{C}^*$  with spin and parity  $J^\pi = \frac{1}{2}^+$  into the photon, neutron, proton, and  $\alpha$  channels are shown as functions of excitation energy. Note that all particle decay channels open at the correct thresholds ( $S_\alpha = 7.54$  MeV,  $S_p = 8.69$  MeV,  $S_n = 13.12$  MeV) because the experimental masses of the involved nuclei have been used. With increasing excitation energy, as soon as a hadronic decay channel opens, the branching for  $\gamma$ -decay (electro-magnetic interaction) becomes negligible. While the contribution to the neutron channel rises immediately after the threshold, the branching into the proton channel needs 2-3 MeV above the threshold to become open because the Coulomb barrier has to be overcome.

If particle emission decay leads to an excited level of the residual nucleus, we again calculate the branching ratios for the subsequent emission with the statistical model (iteration of SMOKER). By keeping track of the energies of the ejected particles and photons during the cascade, and by weighting them with the corresponding branching ratios, the energy spectra for emitted neutrons, protons,  $\alpha$ s, and  $\gamma$ s can be determined. Since the amount of excitation energy in the system is significantly reduced with

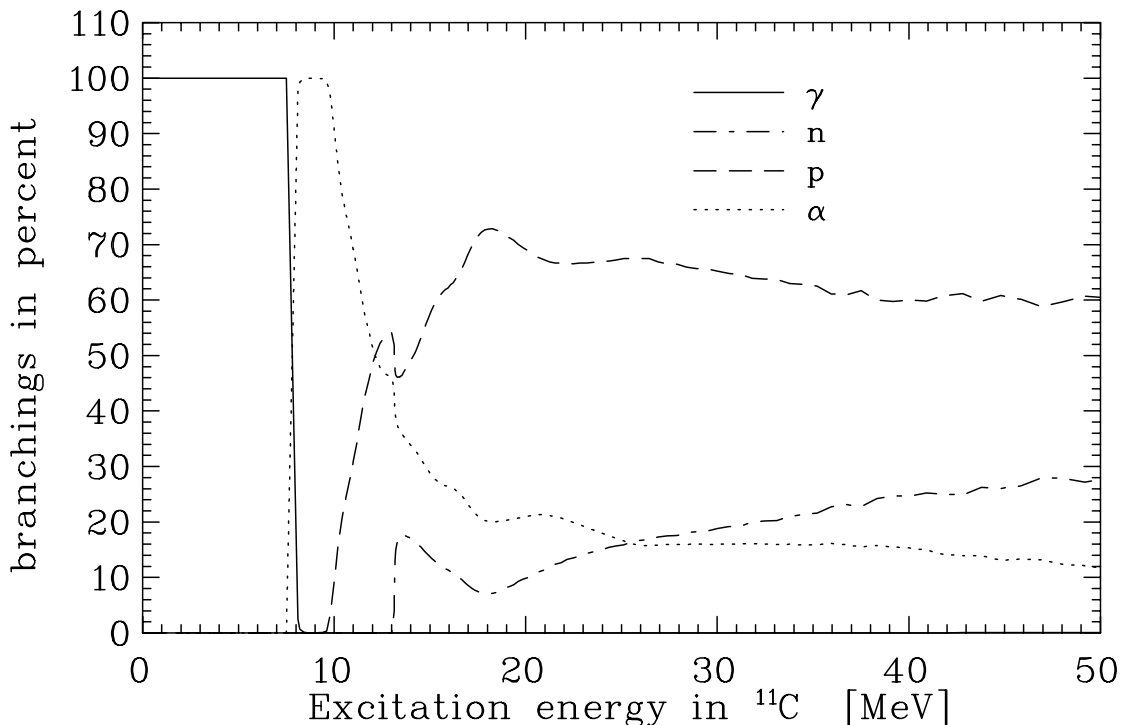


FIG. 2: Energy dependence of de-excitation branching of a  $J^\pi = \frac{1}{2}^+$   $^{11}\text{C}^*$  state by emission of a  $\gamma$ , neutron, proton, or  $\alpha$  particle as built into the statistical model (SMOKER code).

every particle emission and eventually drops below the particle emission thresholds, we found that the cascade could practically be terminated after two emission steps, i.e., the residual daughter nuclei after two iterations were assumed to be in their ground state.

The SMOKER code has been applied extensively to many astrophysical problems, mainly where nuclei with mass number  $A > 20$  are involved. In such a case the requirement of a high level density, which is one of the main assumptions of the statistical model, is usually met, and the calculated cross sections are generally in good agreement with the experimental data [28]. For the light nuclei considered here, an application of the statistical method might seem problematic because the level density in light nuclei can be small, and in many reactions with light nuclei, significant direct contributions have been found. However, by studying the de-excitations of  $^{12}\text{C}$  and  $^{16}\text{O}$  nuclei that had been excited by inelastic neutrino scattering, it was found that the branching ratios for decay into the proton and neutron channels, calculated within the statistical model, were in very good agreement with the branching ratios obtained from a continuum random phase approximation [30]. That means that at certain conditions, direct contributions can be effectively accounted for in the statistical model. Although at specific excitation energies, the branchings calculated within both models deviated by a factor of 2, the proton and neutron branchings averaged over various excitation spectra corresponding to different neutrino energies were found to match within 1-17%. As for our calculations

in this paper, due to the spreading width of the excited state, the branching ratios from the statistical model are also averaged over a range of excitation energies. Therefore, we conservatively adopt the relative error in the branchings for one- and two-step decays to be 20% and 30%, respectively.

We now turn to the results of our calculations of the final states of nuclear de-excitations following the disappearance of a neutron from the  $s_{1/2}$  shell in  $^{12}\text{C}$ . Results of these calculations are shown in Table I. They were obtained for an excited  $J^\pi = \frac{1}{2}^+$  level at  $E^* = 23$  MeV in  $^{11}\text{C}$  with an associated Lorentzian width of  $\Gamma=7$  MeV.

The first upper block in the table just shows the branching ratios for one-step emission into the  $\gamma$ , neutron, proton, and  $\alpha$  channels. In the second block the branching of the first-step neutron channel is divided into the contributions directly to the ground state and the contributions to the excited states in the daughter nucleus  $^{10}\text{C}$ , which undergo subsequent second-step  $\gamma$ , neutron, proton, or  $\alpha$  emission. In the same way, the first-step proton and  $\alpha$  channels are split up in the lower blocks of Table I. In comparison to the time scale relevant for the detection of the ejectiles, the emission of de-excitation particles occurs simultaneously. Hence the “symmetric” channels like  $^{11}\text{C}(n,p)$  and  $^{11}\text{C}(p,n)$  will lead to identical signatures in the detector and therefore we list the sum of these branchings in the lowest block of Table I. Next to the two-step de-excitation mode, shown in the first column of Table I, the residual daughter nu-

TABLE I: Branching ratios for  $^{11}\text{C}^*$  de-excitation modes after a neutron disappears from the  $s_{1/2}$ -state in  $^{12}\text{C}$  and experimental signature (number of time-correlated hits) for observation of these modes in a large liquid scintillator detector. For the final states marked with \*, due to the very large lifetime of the daughter nuclei, the experimental signature is assumed to be a single hit.

Decay mode	Daughter (decay, $T_{1/2}$ or $\Gamma$ , $Q_{EC}$ or $Q_{\beta^-}$ )	Mode %	Exp. sign. (hits)
$^{11}\text{C}(\gamma)$	$^{11}\text{C}_{\text{gs}}(\beta^+; 20.4 \text{ m}, 1.98 \text{ MeV})$	0.7	2
$^{11}\text{C}(\text{n} \dots)$	↓	13.8	↓
$^{11}\text{C}(\text{p} \dots)$	↓	64.4	↓
$^{11}\text{C}(\alpha \dots)$	↓	21.1	↓
$^{11}\text{C}(\text{n})$	$^{10}\text{C}_{\text{gs}}(\beta^+; 19.3 \text{ s}, 3.65 \text{ MeV})$	3.0	3
$^{11}\text{C}(\text{n}, \gamma)$	$^{10}\text{C}_{\text{gs}}(\beta^+; 19.3 \text{ s}, 3.65 \text{ MeV})$	2.8	3
$^{11}\text{C}(\text{n}, \text{n})$	$^9\text{C}(\beta^+; 0.127 \text{ s}, 16.5 \text{ MeV})$	0.06	4
$^{11}\text{C}(\text{n}, \text{p})$	$^9\text{B}(\text{p}+2\alpha; 0.54 \text{ keV}, 1.07 \text{ MeV})$	5.7	2
$^{11}\text{C}(\text{n}, \alpha)$	$^6\text{Be}(2\text{p}+\alpha; 92 \text{ keV}, 4.3 \text{ MeV})$	2.2	2
$^{11}\text{C}(\text{p})$	$^{10}\text{B}(\text{stable})$	2.9	1
$^{11}\text{C}(\text{p}, \gamma)$	$^{10}\text{B}(\text{stable})$	19.0	1
$^{11}\text{C}(\text{p}, \text{n})$	$^9\text{B}(\text{p}+2\alpha; 0.54 \text{ keV}, 1.07 \text{ MeV})$	1.4	2
$^{11}\text{C}(\text{p}, \text{p})$	$^9\text{Be}(\text{stable})$	7.2	1
$^{11}\text{C}(\text{p}, \alpha)$	$^6\text{Li}(\text{stable})$	33.9	1
$^{11}\text{C}(\alpha)$	$^7\text{Be}(\beta^+; 53.3\text{d}, 0.86 \text{ MeV})$	5.2	1*
$^{11}\text{C}(\alpha, \gamma)$	$^7\text{Be}(\beta^+; 53.3\text{d}, 0.86 \text{ MeV})$	4.2	1*
$^{11}\text{C}(\alpha, \text{n})$	$^6\text{Be}(2\text{p}+\alpha; 92 \text{ keV}, 4.3 \text{ MeV})$	0.3	2
$^{11}\text{C}(\alpha, \text{p})$	$^6\text{Li}(\text{stable})$	3.4	1
$^{11}\text{C}(\alpha, \alpha)$	$^3\text{H}(\beta^-; 12.3\text{y}, 18.6 \text{ keV})$	8.0	1*
$^{11}\text{C}\{\text{n}, \text{p}\}$	$^9\text{B}(\text{p}+2\alpha; 0.54 \text{ keV}, 1.07 \text{ MeV})$	7.1	2
$^{11}\text{C}\{\text{n}, \alpha\}$	$^6\text{Be}(2\text{p}+\alpha; 92 \text{ keV}, 4.3 \text{ MeV})$	2.5	2
$^{11}\text{C}\{\text{p}, \alpha\}$	$^6\text{Li}(\text{stable})$	37.3	1

clei are listed in the second column. Some of these nuclei are radioactive and can provide a time-correlated signal with the emitted particles in the detection process. The third column gives branching ratios in percentages per one neutron in the  $s_{1/2}$  state.

Energy spectra for de-excitation  $\gamma$ s and neutrons are shown in Figures 3 and 4 respectively. Figure 3 shows the calculated  $\gamma$ -spectra for all de-excitation modes (dotted line), for  $^{11}\text{C}^*(\gamma)^{11}\text{C}_{\text{gs}}$  transitions (dashed line), and for the transition  $^{11}\text{C}^*(\text{n}, \gamma)^{10}\text{C}_{\text{gs}}$  (solid line). The last spectrum is dominated by a strong monoenergetic line at 3.35 MeV, corresponding to the decay of the first excited  $2^+$  state in  $^{10}\text{C}$ . Figure 4 shows the energy spectra for the emitted neutrons. While the solid line depicts the summed neutron spectra from all processes following the disappearance of a  $s_{1/2}$  neutron, the dotted line just shows the neutron energy distribution from the  $^{11}\text{C}^*(\text{n}, \gamma)^{10}\text{C}_{\text{gs}}$  mode, and the dashed line relates to the neutrons from the decay  $^{11}\text{C}^*(\text{n})^{10}\text{C}_{\text{gs}}$ . The spectrum of neutrons from the  $^{11}\text{C}^*(\text{n}, \gamma)^{10}\text{C}_{\text{gs}}$  mode reflects the width of the initial  $s_{1/2}$  neutron level in  $^{12}\text{C}$ .

In liquid scintillator detectors the emission of de-excitation  $\gamma$ s, protons, and  $\alpha$ s will be seen as a prompt

TABLE II: Branching ratio (in percent) into the  $^{11}\text{C}^*(\text{n}, \gamma)^{10}\text{C}_{\text{gs}}$  decay channel as a function of binding energy and spreading width of  $s_{1/2}$  neutron level in  $^{12}\text{C}$ .

$E_{s_{1/2}}$ [MeV]	$\Gamma_{s_{1/2}}$ [MeV]					
	6	7	8	10	12	15
40.7	2.90	2.76	2.65	2.46	2.31	2.14
41.7	2.97	2.84	2.73	2.54	2.38	2.20
42.7	2.97	2.85	2.75	2.57	2.42	2.24

signal, and we assumed here that these particles cannot be distinguished. The neutrons, although emitted at the same time as other de-excitation products, will result in a double signal. First, they will quickly slow down by elastic collisions with hydrogen (which, besides  $^{12}\text{C}$ , is another essential component of the liquid scintillator) and thus will also contribute to the prompt component of the signal. Second, thermalized neutrons will diffuse in the liquid scintillator for typically 200  $\mu\text{sec}$  before they are captured by hydrogen atoms with emission of a detectable 2.2 MeV photon. Thus, neutrons can provide two signals in the chain of detected events. Residual radioactive nuclei left after one- or two-particle de-excitations will provide another signal in the chain of events initiated by the disappearance of the neutron, all coming from the same point in the detector within the reconstruction space resolution and within certain correlation time. We also note that positrons from  $\beta^+$  decay of the daughter nuclei in Table I can be seen in the liquid scintillator detector with efficiency close to 100%.

The chain of time- and space-correlated events creates a unique signature for the detection of neutron disappearance in low-threshold liquid scintillator detectors. The right-most column of Table I shows the experimental signatures of the corresponding decay modes in terms of time- and space-correlated hits in the detector. One can see that the decay chains:  $^{11}\text{C}^* \rightarrow \text{n} + \gamma + ^{10}\text{C}_{\text{gs}}$ , with a branching of 2.8%,  $^{11}\text{C}^* \rightarrow \text{n} + ^{10}\text{C}_{\text{gs}}$ , with a branching of 3.0%, and  $^{11}\text{C}^* \rightarrow \text{n} + \text{n} + ^9\text{C}_{\text{gs}}$ , with a branching of 0.06% provide 3-hit or 4-hit signatures. Therefore these decay modes should be very immune to possible accidental-coincidence background.

As the initial values for the excitation energy  $E^*$  and spreading width  $\Gamma$  are not precisely known, in order to estimate the corresponding systematic stability of our results, we varied these quantities within their uncertainty range:  $\pm 1$  MeV for  $E^*$  and from 6 MeV to 15 MeV for  $\Gamma$ . Exemplary for all decay modes, the effect of the variations on the results are shown in Table II for the branching to the  $^{11}\text{C}^* \rightarrow \text{n} + \gamma + ^{10}\text{C}_{\text{gs}}$  channel, which we consider to deliver the most robust signature for a neutron disappearance.

One can see from Table II that the predicted branching ratio is rather insensitive to the variation of  $E^*$  and  $\Gamma$ . Since, as mentioned above, an error of 30% should be assigned to the branching ratios, we consider the system-

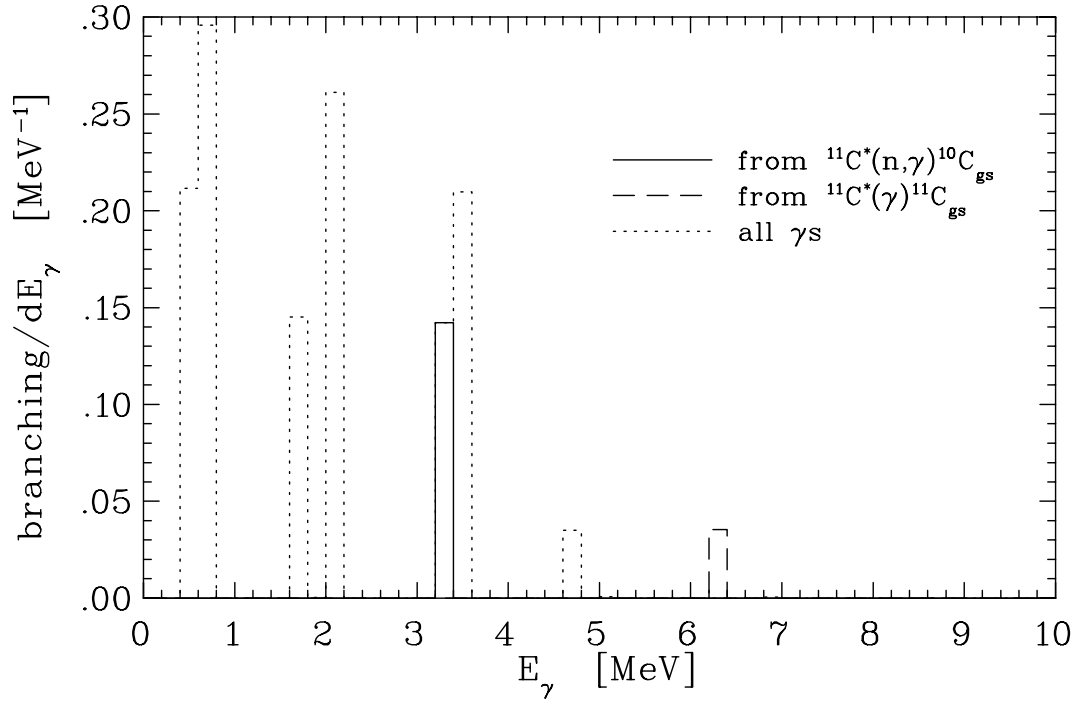


FIG. 3: Spectra of  $\gamma$ s from de-excitations of  $s_{1/2}$  hole of neutron disappearance in  $^{12}\text{C}$ . The dotted line is for all  $\gamma$ s from all de-excitation processes; the dashed line is for  $^{11}\text{C}^*(\gamma)^{11}\text{C}_{gs}$  transition, and the solid line is for the de-excitation mode  $n + \gamma$  with a residual  $^{10}\text{C}_{gs}$  nucleus. The energy bin width is 0.2 MeV.

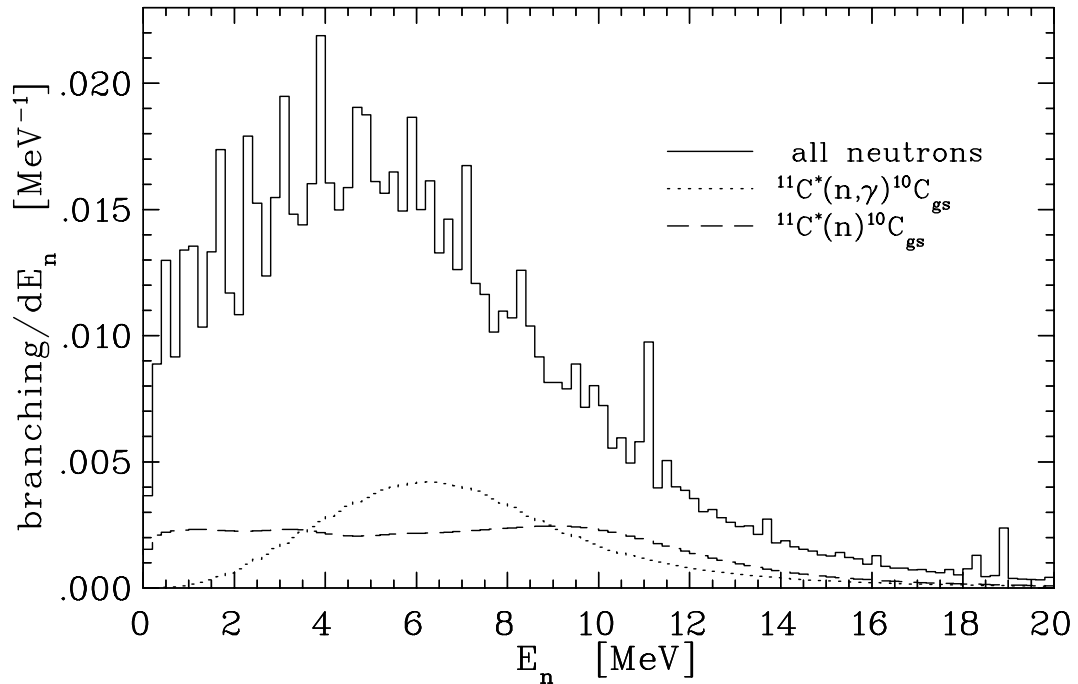


FIG. 4: Spectra of neutrons from de-excitations of  $s_{1/2}$  hole of neutron disappearance in  $^{12}\text{C}$ . The solid line is for all neutrons from all de-excitation processes; the dotted line is for the process with emission of de-excitation  $n, \gamma$ , and  $^{10}\text{C}_{gs}$  residual nucleus; the dashed line is for the process with de-excitation via emission of neutron and  $^{10}\text{C}_{gs}$  residual nucleus. The energy bin width is 0.2 MeV.

atic error coming from the uncertainty in  $E^*$  and  $\Gamma$  to be negligible.

In this paper we assume that decay products on neutron disappearance (e.g.  $n \rightarrow \nu\bar{\nu}$ ) have total momentum equal to the momentum of the initial neutron. That can be justified by the assumption that disappearance of a neutron occurs at very short distances and for very short times relative to the distances and times that are characteristic of nuclear processes. Therefore, one can expect that the momentum of the disappearing neutron is taken away by the decay products except possibly for a small recoil given to the residual nucleus as a whole. Our main result, the branching ratios for the residual nucleus de-excitation, will not be affected by the recoil motion. However, spectra of emitted protons,  $\alpha$ s, and neutrons might be smeared out by this motion. From experimental point of view this smearing will not lead to any principal effects, it might only slightly increase the uncertainty of the efficiency of detection of these particles due to the finite visible energy threshold.

#### IV. NEUTRON DISAPPEARANCE FROM $^{16}\text{O}$

Neutron disappearance from the  $s_{1/2}$  state in  $^{16}\text{O}$  followed by  $\gamma$  de-excitation from a highly excited state has been considered in [17] for a Kamiokande experiment with a water-Čerenkov detector. The branching ratio for this de-excitation mode was calculated in this paper. It is interesting to compare our branching ratio calculations for the initial  $^{12}\text{C}$  nucleus with this result. Integrating  $\gamma$  spectrum of  $^{11}\text{C}^*$  de-excitation, which is shown in Figure 3 as a dotted line, within the energy range from 19 to 50 MeV, as suggested by Ref. [17], we found a branching ratio of  $1.1 \cdot 10^{-4}$ . This is similar to the  $s_{1/2}$  hole  $\gamma$  de-excitation branching ratio in  $^{16}\text{O}$ , calculated in [17] as  $(0.27 - 1.04) \cdot 10^{-4}$ .

We have also calculated the spectrum of final de-excitation states for an excited  $^{15}\text{O}$  nucleus, originated by a neutron hole in the  $S_{1/2}$  neutron level in  $^{16}\text{O}$ . These branching ratios are shown in Table III. They were obtained by SMOKER code calculations assuming the values  $E^* = 29$  MeV and  $\Gamma = 7$  MeV respectively for the energy and spreading width of the excited state in  $^{15}\text{O}$ .

Figure 5 shows in a logarithmic scale the spectrum of  $\gamma$ s from  $S_{1/2}$  de-excitations of  $^{15}\text{O}^*$ . For the  $\gamma$  branching ratio, integrated over the energy range 19–50 MeV, we obtain the value  $1.4 \cdot 10^{-4}$ . By varying the energy level and width of the  $s_{1/2}$  state in  $^{16}\text{O}$  by  $\pm 1$  MeV, we found the branching to change in the range  $(1.3-1.5) \cdot 10^{-4}$ . Furthermore, taking into account the uncertainty in the threshold energy of 19 MeV due to the energy scale calibration of  $\pm 0.6$  MeV, the range becomes  $(1.2-1.6) \cdot 10^{-4}$ . Finally, estimating the systematic uncertainties of the SMOKER code, we conclude that  $\gamma$  branching for de-excitation of the  $S_{1/2}$  hole in  $^{16}\text{O}$  within the energy range 19–50 MeV is  $(1.4 \pm 0.7) \cdot 10^{-4}$ , which is in good agreement with the result  $(0.27-1.04) \cdot 10^{-4}$  of the calculations

TABLE III: Branching ratios for  $^{15}\text{O}^*$  de-excitation after neutron disappearance from a  $s_{1/2}$  hole state in  $^{16}\text{O}$ .

Decay mode	Daughter (decay, $T_{1/2}$ or $\Gamma$ , $Q_{EC}$ )	Mode %
$^{15}\text{O}(\gamma)$	$^{15}\text{O}_{gs}(\beta^+; 122.2\text{s}, 2.75 \text{ MeV})$	0.5
$^{15}\text{O}(n\dots)$	$\downarrow$	14.2
$^{15}\text{O}(p\dots)$	$\downarrow$	64.3
$^{15}\text{O}(\alpha\dots)$	$\downarrow$	21.0
$^{15}\text{O}(n)$	$^{14}\text{O}_{gs}(\beta^+; 70.6\text{s}, 5.14 \text{ MeV})$	1.1
$^{15}\text{O}(n,\gamma)$	$^{14}\text{O}_{gs}(\beta^+; 70.6\text{s}, 5.14 \text{ MeV})$	0.0
$^{15}\text{O}(n,n)$	$^{13}\text{O}(\beta^+; 8.58\text{ms}, 17.8 \text{ MeV})$	0.0
$^{15}\text{O}(n,p)$	$^{13}\text{N}(\beta^+; 9.97\text{s}, 2.22 \text{ MeV})$	12.6
$^{15}\text{O}(n,\alpha)$	$^{10}\text{C}(\beta^+; 19.3\text{s}, 3.65 \text{ MeV})$	0.5
$^{15}\text{O}(p)$	$^{14}\text{N}(\text{stable})$	3.4
$^{15}\text{O}(p,\gamma)$	$^{14}\text{N}(\text{stable})$	10.4
$^{15}\text{O}(p,n)$	$^{13}\text{N}(\beta^+; 9.97\text{s}, 2.22 \text{ MeV})$	11.3
$^{15}\text{O}(p,p)$	$^{13}\text{C}(\text{stable})$	30.4
$^{15}\text{O}(p,\alpha)$	$^{10}\text{B}(\text{stable})$	8.8
$^{15}\text{O}(\alpha)$	$^{11}\text{C}(\beta^+; 20.4\text{m}, 1.98 \text{ MeV})$	1.4
$^{15}\text{O}(\alpha,\gamma)$	$^{11}\text{C}(\beta^+; 20.4\text{m}, 1.98 \text{ MeV})$	6.0
$^{15}\text{O}(\alpha,n)$	$^{10}\text{C}(\beta^+; 19.3\text{s}, 3.65 \text{ MeV})$	0.4
$^{15}\text{O}(\alpha,p)$	$^{10}\text{B}(\text{stable})$	4.5
$^{15}\text{O}(\alpha,\alpha)$	$^7\text{Be}(\beta^+; 53.3\text{d}, 0.86 \text{ MeV})$	8.7
$^{15}\text{O}\{n,p\}$	$^{13}\text{N}(\beta^+; 9.97\text{s}, 2.22 \text{ MeV})$	23.9
$^{15}\text{O}\{n,\alpha\}$	$^{10}\text{C}(\beta^+; 19.3\text{s}, 3.65 \text{ MeV})$	0.9
$^{15}\text{O}\{p,\alpha\}$	$^{10}\text{B}(\text{stable})$	13.3

from Ref. [17].

#### V. TWO-NEUTRON DISAPPEARANCE FROM $^{12}\text{C}$

Since the disappearance of two neutrons would be a process occurring at a very short distance, we should consider both disappearing neutrons to be in the same subshell, and thus we will neglect the cases when one S-shell and one P-shell neutrons are disappearing together.

##### A. Disappearance from the $p_{1/2}$ or $p_{3/2}$ shell

In the simple shell-model picture, a disappearance of two neutrons from the  $p_{3/2}$  shell would always lead to  $J^\pi = 0^+$  ground state of  $^{10}\text{C}$ . However, due to correlations and particularly due to nucleon pairing, as was discussed earlier, there is a probability of  $\sim 40\%$  of finding a pair of neutrons in the  $p_{1/2}$  level. We again assume that the disappearance of two neutrons would occur due to a very short-range interaction, and therefore expect the disappearance of paired neutrons in either a  $p_{1/2}$  or a  $p_{3/2}$  state to be more likely than the disappearance of a pair of one  $p_{1/2}$  and one  $p_{3/2}$  neutrons. Nevertheless, we will discuss both cases below.



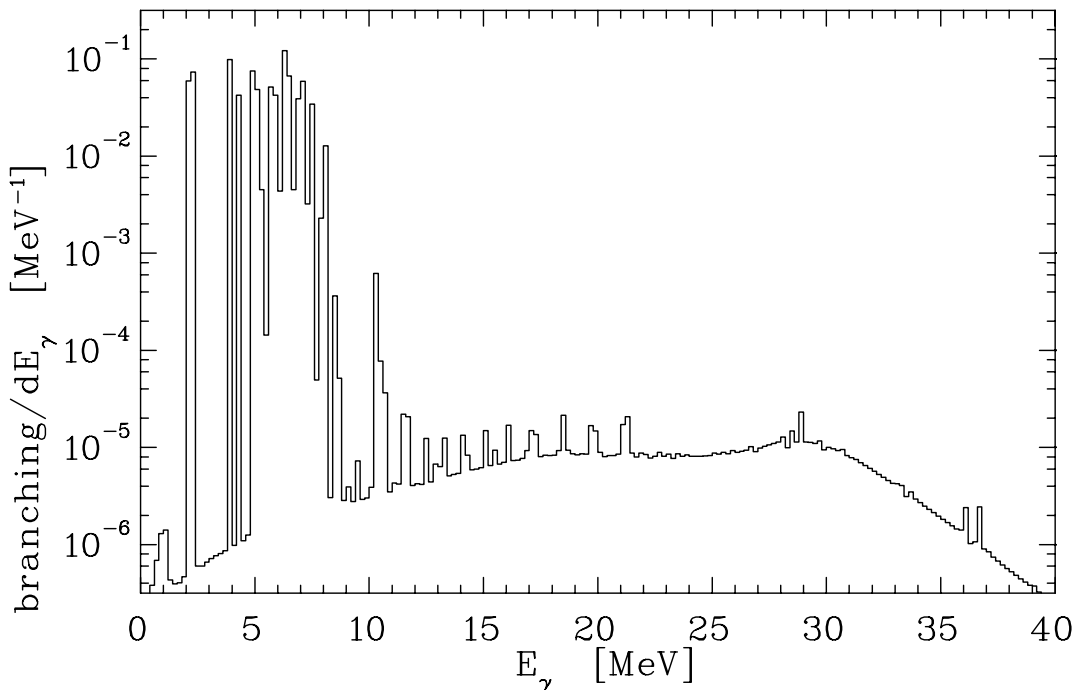


FIG. 5: Spectrum of  $\gamma$ s from de-excitation of a  $s_{1/2}$  hole resulting from neutron disappearance in  $^{16}\text{O}$ . The energy bin width is 0.2 MeV.

The disappearance of paired neutrons with total spin 0 would imply certain selection rules for the final state of disappearance. Thus, from the conservation of angular momentum, the transition  $nn \rightarrow \nu\bar{\nu}$  with  $\Delta(B-L) = -2$  is possible while transitions  $nn \rightarrow \nu\nu$  or  $nn \rightarrow \bar{\nu}\bar{\nu}$  are not. The disappearance of two neutrons from the  $p_{1/2}$  level will lead to the ground state of  $^{10}\text{C}$ . The disappearance of two neutrons from a  $p_{3/2}$  state, while two other neutrons are in a  $p_{1/2}$  state, might result in the excited state of  $^{10}\text{C}$  with  $J^\pi = 0^+$ . Since there are no excited states of  $^{10}\text{C}$  with this spin and parity below the proton separation threshold, the residual de-excitation will be dominated by  $^{10}\text{C}^* \rightarrow p+^9\text{B}$ , and  $^9\text{B}$  will quickly decay into  $p + 2\alpha$ . Such de-excitation will lead only to a single-hit signature in the liquid scintillator detector and therefore is not favorable for detection.

A disappearance of one  $p_{3/2}$  and one  $p_{1/2}$  neutron would lead to an excited state in  $^{10}\text{C}$  with spin and parity  $J^\pi = 2^+$  or  $1^+$ . There is not any low lying energy level known in  $^{10}\text{C}$  with spin and parity  $1^+$  [24]. However, there are 3 low lying energy levels stated in  $^{10}\text{C}$  (two are well established and one is assumed) with spin and parity  $2^+$  [24] that could be populated after 2-neutron disappearance. To our knowledge, no experimental or theoretical information on the spectroscopic factors for these possible final states exists here. However, as 2 out of the three excited  $2^+$  states in  $^{10}\text{C}$  lie above the proton or even  $\alpha$  separation threshold, their decay will proceed by emission of a low energetic proton or  $\alpha$ -particle, leading to the  $^9\text{B}$  and  $^6\text{Be}$  ground states, respectively. As  $^9\text{B}$

immediately decays into a proton and two  $\alpha$  particles, and the  $^6\text{Be}$  into 2 protons and  $\alpha$ , this will lead only to a single-hit signature in the liquid scintillator detector. Only the population of the first excited  $2^+$  state at 3.35 MeV will produce a space and time correlated two-hit event in the detector. This state decays by emission of a photon with energy 3.35 MeV, followed by the  $\beta^+$  decay of the residual  $^{10}\text{C}_{gs}$  with a correlation time of 27.8 s and detectable energy between 1.74 and 3.65 MeV. As an upper limit for the probability of this event we adopt the value 40 percent  $\times$  4/6 (probability to pick a  $(p_{3/2}, p_{1/2})$  pair from two  $p_{3/2}$  and two  $p_{1/2}$  neutrons) / 3 (number of low lying  $2^+$  states in  $^{10}\text{C}$ ) or 9 % per  $^{12}\text{C}$  atom, with an estimated error of  $\pm 5$  %.

## B. Disappearance from the $s_{1/2}$ shell

For the disappearance of two neutrons from the  $s_{1/2}$  state, we estimated the excitation energy of  $^{10}\text{C}^*$  in the following way: bound energy of two neutrons in the  $s_{1/2}$  state is assumed as 78 MeV; separation energy of two neutrons from  $^{12}\text{C}$  is 31.8 MeV; thus the excitation energy is  $\sim 46$  MeV. With respect to the spreading width of a double  $s_{1/2}$  hole state one might be inclined to assume that it should be larger than the width of a single  $s_{1/2}$  hole (7 MeV). However, essential contribution to the spreading width of the single  $s_{1/2}$  hole is due to the pairing correlations that should be significantly reduced for a double  $s_{1/2}$  hole state. Therefore, a width of

$\Gamma=7$  MeV has been assumed for a double  $s_{1/2}$  hole state. The results of SMOKER code calculations for this case are shown in Table IV and were found to change their relative value by less than 3.5 percent when varying the spreading width between  $\Gamma=4$  and 15 MeV.

There are two final-state modes in this table that would result in a 3-hit event signature in the liquid scintillator detector, each with a branching of about 6% per S-shell neutron. Figure 6 shows the energy spectra of neutrons for these de-excitation modes. Note that both spectra reflect an initial Lorentz-shape distribution of excitation energy. For the mode  $^{10}\text{C}^* \rightarrow n + p + ^8\text{B}_{gs}$ , the proton, which comes from the decay of the first excited state in  $^9\text{C}$ , is monoenergetic with energy 0.922 MeV.

## VI. DISCUSSION

The KamLAND detector [2] is perfectly suited to search for the neutron disappearance processes in carbon, i.e., for the observation of sequences of nuclear de-excitation events. The active mass of the KamLAND detector filled with a liquid scintillator (formula  $\sim \text{CH}_2$ ) is  $\sim 900$  tons; the trigger threshold can be as low as  $\sim 0.2$  MeV; the photon energy resolution at 1 MeV is  $\leq 8\%$ . Good time and energy resolution allow reconstruction of

TABLE IV: Branching ratios for  $^{10}\text{C}^*$  de-excitation after two-neutron disappearance from  $s_{1/2}$ -state of  $^{12}\text{C}$ .

Decay mode	Daughter (decay, $T_{1/2}$ or $\Gamma$ , $Q_{EC}$ )	Mode %	Exp. sign. (hits)
$^{10}\text{C}(\gamma)$	$^{10}\text{C}_{gs}(\beta^+, 19.3 \text{ s}, 3.65 \text{ MeV})$	0.0	-
$^{10}\text{C}(n \dots)$	$\downarrow$	12.2	$\downarrow$
$^{10}\text{C}(p \dots)$	$\downarrow$	63.7	$\downarrow$
$^{10}\text{C}(\alpha \dots)$	$\downarrow$	24.1	$\downarrow$
$^{10}\text{C}(n)$	$^9\text{C}(\beta^+, 0.127 \text{ s}, 16.5 \text{ MeV})$	6.2	3
$^{10}\text{C}(n, \gamma)$	$^9\text{C}$	0.0	-
$^{10}\text{C}(n, n)$	$^8\text{C}$	0.0	-
$^{10}\text{C}(n, p)$	$^8\text{B}(\beta^+ \alpha, 770 \text{ ms}, 18 \text{ MeV})$	6.0	3
$^{10}\text{C}(n, \alpha)$	$^5\text{Be}$	0.0	-
$^{10}\text{C}(p)$	$^9\text{B}$	0.0	-
$^{10}\text{C}(p, \gamma)$	$^9\text{B}$	0.0	-
$^{10}\text{C}(p, n)$	$^8\text{B}$	0.0	-
$^{10}\text{C}(p, p)$	$^8\text{Be}(2\alpha, 6.8 \text{ eV}, Q_\alpha=92 \text{ keV})$	27.3	1
$^{10}\text{C}(p, \alpha)$	$^5\text{Li}(p+\alpha, 1.5 \text{ MeV}, Q_p=1.97 \text{ MeV})$	36.4	1
$^{10}\text{C}(\alpha)$	$^6\text{Be}(2p+\alpha, 92 \text{ keV}, Q_{p\alpha}=1.37 \text{ MeV})$	8.7	1
$^{10}\text{C}(\alpha, \gamma)$	$^6\text{Be}$	0.0	-
$^{10}\text{C}(\alpha, n)$	$^5\text{Be}$	0.0	-
$^{10}\text{C}(\alpha, p)$	$^5\text{Li}(p+\alpha, 1.5 \text{ MeV}, Q_p=1.97 \text{ MeV})$	14.1	1
$^{10}\text{C}(\alpha, \alpha)$	$^2\text{H}(\text{stable})$	1.3	1
$^{10}\text{C}\{n, p\}$	$^8\text{B}(\beta^+ \alpha, 770 \text{ ms}, 18 \text{ MeV})$	6.0	3
$^{10}\text{C}\{n, \alpha\}$	$^5\text{Be}$	0.0	-
$^{10}\text{C}\{p, \alpha\}$	$^5\text{Li}(p+\alpha, 1.5 \text{ MeV}, Q_p=1.97 \text{ MeV})$	50.5	1

an event position in the detector with the accuracy down to several cm. Low background in the KamLAND experiment is due to a deep underground location (2,700 meters of water equivalent), water shield, buffer oil shield, veto system, radon shields, and liquid scintillator purification that provide concentration of  $^{238}\text{U}$ ,  $^{232}\text{Th}$ , and  $^{40}\text{K}$  at the level below  $10^{-15}$  g/g [29].

## Experimental signatures

We have calculated in sections III and V above the branching ratios for various de-excitations following the disappearance of one or two neutrons from the  $^{12}\text{C}$  nucleus. Not all de-excitation modes are favorable for detection in the experiment, but some of them form the chains of time- and space-correlated events in the detector. Thus, the process  $^{11}\text{C}^* \rightarrow n + \gamma + ^{10}\text{C}_{gs}$  from the disappearance of a neutron from the  $s_{1/2}$  state will look like a 3-hit event in the detector. The first hit in the detector will be produced by monoenergetic  $\gamma$ s with an energy of 3.35 MeV corresponding to the de-excitation of a  $2^+$  level of  $^{10}\text{C}$  and by slow-down interactions of neutron in the scintillator. The first hit will be followed by a second hit, which is due to neutron capture by hydrogen in the scintillator (correlation time is  $\sim 200\mu\text{sec}$ ). The third hit will be due to delayed  $\beta^+$  decay of  $^{10}\text{C}_{gs}$  with correlation time 27.8 sec and detectable energy in the range 1.74–3.65 MeV. The first two hits will look similar to a signature of the reactor antineutrino interactions: positron plus delayed captured neutron. The detection of reactor antineutrinos is the main purpose of the KamLAND experiment [2]. The expected number of reactor antineutrino interactions in KamLAND in the absence of neutrino oscillations is  $\sim 600$  per kt per year with the background less than few percent [2]. Using the measurements performed in the KamLAND Collaboration [29], one can conservatively estimate the background for an accidental 3-hit coincidence (first hit with a threshold of 2.8 MeV, second hit with a threshold of 1.6 MeV; window for first two hits is 0.54 msec; threshold for the third hit is 2 MeV; time window for the third hit is 60 sec; position-correlation cut of  $\sim 1\text{m}$ ) to be below one event per year. This accidental background rate can be measured in the detector and subtracted. Using branching for  $^{11}\text{C}^* \rightarrow n + \gamma + ^{10}\text{C}_{gs}$  from Table I and assuming no other sources of events with such a signature (e.g. from atmospheric neutrino interactions), for one year of exposition time in the KamLAND detector, one can, with 90% CL, set a limit for  $n \rightarrow \nu\nu\bar{\nu}$  decay at the level  $5 \cdot 10^{29}$  years. This is 1,000 times better than the present limit for this decay mode [1].

Detection of the 3-hit process  $^{11}\text{C}^* \rightarrow n + ^{10}\text{C}_{gs}$  will be similar to the one discussed above, probably with a different threshold for the first hit that will be formed by the slow-down interactions of neutrons in the liquid scintillator. Detection of the 4-hit process  $^{11}\text{C}^* \rightarrow n + n + ^9\text{C}_{gs}$  would be a spectacular observation; unfortunately its

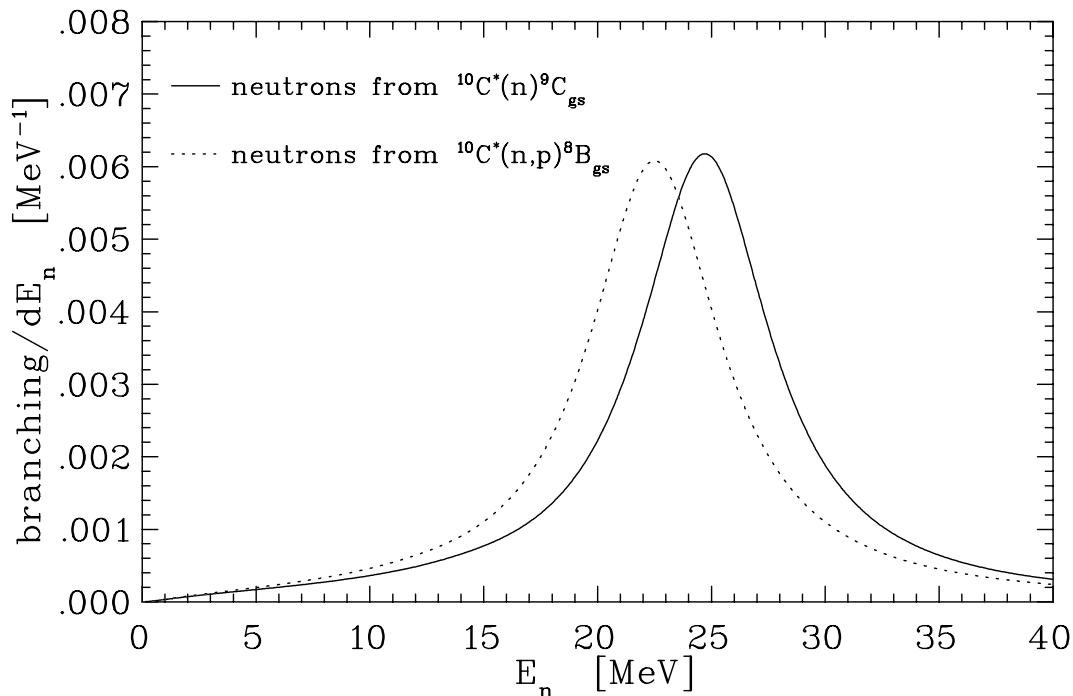


FIG. 6: Energy spectrum of neutrons from de-excitations of a  $s_{1/2}$  hole resulting from two-neutron disappearance in  $^{12}\text{C}$ . The solid line is for transition  $^{10}\text{C}^* \rightarrow n + ^9\text{C}_{gs}$  and the dotted line is for  $^{10}\text{C}^* \rightarrow n + p + ^8\text{B}_{gs}$ . The energy bin width is 0.2 MeV.

branching, as follows from Table I, is much lower than for two processes with the 3-hit signature discussed above.

The two-hit events listed in Table I should be divided into two categories. Events with one of the de-excitation particles being a neutron belong to the first category; in KamLAND these events will have a signature similar to that for anti-neutrino reactor events with a corresponding background and will be difficult to disentangle. The second category should include events with radioactive daughter nuclei. Events resulting from the neutron disappearance from the  $p_{3/2}$  state of  $^{12}\text{C}$  should also belong in this category. Accidental coincidence background will be more of a problem for the events with long lifetime daughter isotopes therefore only modes with a production of  $^{11}\text{C}_{gs}$  might have practical interest for the detection. Correlation time between two hits in this case is 20.4 min due to lifetime of  $^{11}\text{C}_{gs}$ . The statistical fluctuations of the background will determine the sensitivity limit for a corresponding process search. Optimistically, this measurement alone can improve the existing lifetime limit for  $n \rightarrow \nu\nu\bar{\nu}$  by approximately an order of magnitude.

De-excitation final states originated by the disappearance of two neutrons from  $^{12}\text{C}$  provide two interesting 3-hit signatures:  $^{10}\text{C}^* \rightarrow n + ^9\text{C}_{gs}$  with a branching of 6.2% and  $^{10}\text{C}^* \rightarrow n + p + ^8\text{B}$  with a branching of 6.0%. The relatively short lifetime of the daughter nuclide makes such events free of accidental background.

### Non-accidental background

It is interesting to see whether atmospheric neutrino events can provide a signature similar to  $^{11}\text{C}^* \rightarrow n + \gamma + ^{10}\text{C}_{gs}$ ,  $^{11}\text{C}^* \rightarrow n + ^{10}\text{C}_{gs}$ , or other processes. We anticipate in the future to study this interesting question in a separate paper treating nuclear de-excitations produced by atmospheric neutrinos and anti-neutrinos in  $^{12}\text{C}$ . Such a study will also be interesting from the point of view of identification of atmospheric neutrino and anti-neutrino interactions in liquid scintillator detectors through the detection of associated nuclear chains of de-excitations and radio-nuclide decays. In the respect of the background for one-neutron or two-neutron disappearance addressed in this paper, few qualitative comments can be made here. Charged current atmospheric neutrino reactions have a rate of about 100 interactions per kt-detector per year. Due to the relatively high energy spectrum of atmospheric neutrinos, leptons produced in charged current interactions usually have an energy larger than the energy typical for nucleus de-excitation. We remind the reader that in the Kamiokande experiment [17] the energy range between 19–50 MeV was practically free of background. Thus, one can hope that charge current processes initiated by atmospheric neutrinos will not produce significant background for neutron disappearance processes, i.e., the chain of events with the first signal in a few-MeV range. However, detailed simulations of atmospheric neutrino interactions with  $^{12}\text{C}$  using the SMOKER code for treatment of nuclear de-excitations

are needed to understand this background quantitatively. In such simulations, the production of low energy charged leptons has to be estimated together with de-excitation of  $^{12}\text{N}^*$  and  $^{12}\text{B}^*$  nuclei with a continuous spectrum of excitations. Neutral current atmospheric neutrino interactions should be also followed by de-excitations of  $^{12}\text{C}^*$  (see paper [31]) and might, for example, potentially lead to the process  $^{12}\text{C}^* \rightarrow n + n + \gamma + ^{10}\text{C}_{gs}$  with one of the neutrons lost at the edge of the fiducial volume of the detector.

## VII. CONCLUSIONS

In this paper we show that modern high-mass, low-threshold, and low-background liquid scintillator detectors can observe unique signatures of chains of time- and space-correlated events, formed by nuclear de-excitations following the neutron or two-neutron disappearance from the nucleus. The KamLAND detector [2] is perfectly suited to search for such processes originating from  $^{12}\text{C}$  nuclei. The sensitivity of search for a neutron disappearance (e.g.  $n \rightarrow \nu\nu\bar{\nu}$ ) or two-neutron disappearance (e.g.  $nn \rightarrow \nu\bar{\nu}$ ) in the KamLAND detector can be extended by 3-4 orders of magnitude relative to the present lifetime limits for these processes. Non-accidental back-

ground for neutron and two-neutron disappearance from atmospheric neutrino interactions, although expected to be small, needs to be calculated in future work. Assuming that nucleons can decay only into known particles with conservation of electric charge, 4-momentum, and angular momentum, the search for intra-nucleus neutron and two-neutron disappearance in KamLAND can lead either to the discovery of long-awaited baryon instability or to the improvement of the mode-independent nucleon decay lifetime limit from the present  $1.6 \cdot 10^{25}$  years to or above  $\sim 10^{30}$  years.

We think that the calculations performed in this paper with regard to the KamLAND detector and  $^{12}\text{C}$  nuclei can be extended to other high-mass, low-threshold, and low-background detectors using different nuclei. We plan to continue exploring these possibilities.

## ACKNOWLEDGMENTS

We thank F.-K. Thielemann for providing us with the SMOKER code. We are grateful to Petr Vogel, Andreas Piepke, and Robert Svoboda for useful discussions and critical remarks. Oak Ridge National Laboratory is managed by UT-Battelle, LLC for the U.S. Department of Energy under contract DE-AC05-00OR22725.

- 
- [1] K. Hagiwara *et al.* [Particle Data Group Collaboration], "Review Of Particle Physics," *Phys. Rev. D* **66**, 010001 (2002).
- [2] P. Alivisatos *et al.*, "KamLAND: A liquid scintillator anti-neutrino detector at the Kamioka site," STANFORD-HEP-98-03, Tohoku-RCNS-98-15; K. Eguchi *et al.* [KamLAND Collaboration], "First results from KamLAND: Evidence for reactor anti-neutrino disappearance," *Phys. Rev. Lett.* **90**, 021802 (2003).
- [3] A. D. Sakharov, "Violation of CP Invariance, C Asymmetry, and Baryon Asymmetry of the Universe," *Pisma Zh. Eksp. Teor. Fiz.* **5**, 32 (1967) [*JETP Lett.* **5**, 24 (1967)].
- [4] J. C. Pati and A. Salam, "Unified Lepton - Hadron Symmetry And A Gauge Theory of The Basic Interactions," *Phys. Rev.* **D8**, 1240 (1973); "Is Baryon Number Conserved?," *Phys. Rev. Lett.* **31**, 661 (1973); "Lepton Number as the Fourth Color," *Phys. Rev.* **D10**, 275 (1974).
- [5] H. Georgi and S. L. Glashow, "Unity Of All Elementary Particle Forces," *Phys. Rev. Lett.* **32**, 438 (1974).
- [6] M. Goldhaber, "Search for Nucleon Instability (Origin and History), in *Proceedings of International Workshop on Future Prospects of Baryon Instability Search in p-Decay and  $n \rightarrow \bar{n}$  Oscillation Experiments*, Oak Ridge, Tennessee, pp 1-6 (1996).
- [7] K. S. Babu, J. C. Pati and F. Wilczek, "Fermion masses, neutrino oscillations, and proton decay in the light of SuperKamiokande," *Nucl. Phys.* **B566**, 33 (2000).
- [8] K. S. Babu and R. N. Mohapatra, "Observable neutron anti-neutron oscillations in seesaw models of neutrino mass," *Phys. Lett.* **B518**, 269 (2001).
- [9] Y. Hayato *et al.* [SuperKamiokande Collaboration], "Search for proton decay through  $p \rightarrow \bar{\nu}K^+$  in a large water Čerenkov detector," *Phys. Rev. Lett.* **83**, 1529 (1999); M. Shiozawa *et al.* [SuperKamiokande Collaboration], "Search for proton decay via  $p \rightarrow e^+\pi^0$  in a large water Čerenkov detector," *Phys. Rev. Lett.* **81**, 3319 (1998).
- [10] M. Smy, "Super Kamiokande," invited talk at NNN'01 Workshop, Louisiana State University, Baton Rouge, December 10-12, 2001.
- [11] R. I. Steinberg and J. C. Evans, "Nucleon Stability: A Geochemical Test Independent of Decay Mode," *Science* **197**, 989 (1977).
- [12] J. C. Pati, "Nucleon Decays Into Lepton + Lepton + Anti-Lepton + Mesons Within SU(4) Of Color," *Phys. Rev.* **D29**, 1549 (1984).
- [13] Yu. Kamyshev, "Nucleon instability and (B-L) non-conservation," in *Proceedings of Stony Brook 1999 Workshop on Next Generation Nucleon Decay and Neutrino Detector*, pp 84-87 (1999).
- [14] G. Feinberg, M. Goldhaber and G. Steigman, "Multiplicative Baryon Number Conservation And The Oscillation Of Hydrogen Into Anti-Hydrogen," *Phys. Rev.* **D18**, 1602 (1978).
- [15] Y. Totsuka, in *Proceedings of the 7th Workshop on Grand Unification/ICOBAN '86*, edited by J. Arafune (World Scientific, Singapore, 1986), p. 118.
- [16] H. Ejiri, "Nuclear Deexcitations Of Nucleon Holes Associated With Nucleon Decays In Nuclei," *Phys. Rev. C* **48**, 1442 (1993).
- [17] Y. Suzuki *et al.* [Kamiokande Collaboration], "Study of invisible nucleon decay,  $n \rightarrow \nu\nu\bar{\nu}$ , and a forbidden nu-

- clear transition in the Kamiokande detector,” Phys. Lett. **B311**, 357 (1993).
- [18] R. Bernabei *et al.*, “Search For The Nucleon And Dinucleon Decay Into Invisible Channels,” Phys. Lett. **B493**, 12 (2000).
- [19] J. Learned, F. Reines and A. Soni, “Limits On Nonconservation Of Baryon Number,” Phys. Rev. Lett. **43**, 907 (1979); [Erratum-*ibid.* **43**, 1626 (1979)].
- [20] C. Berger *et al.* [Frejus Collaboration], “Lifetime limits on (B-L) violating nucleon decay and dinucleon decay modes from the Frejus experiment,” Phys. Lett. B **269**, 227 (1991).
- [21] J. F. Glicenstein, “New limits on nucleon decay modes to neutrinos,” Phys. Lett. B **411**, 326 (1997).
- [22] C. Arpesella *et al.*, Borexino Proposal, Vol 1 and 2, ed. G. Bellini and R. S. Raghavan, Univ. of Milan, (1991).
- [23] N. Auerbach, N. Van Giai, and O.K. Vorov, Phys. Rev. C **56** R2368 (1997); E. Kolbe, K. Langanke, and P. Vogel, Nucl. Phys. **A652**, 91-100 (1999); David Dean, Oak Ridge National Laboratory, Private Communication.
- [24] F. Ajzenberg-Selove, Nucl. Phys. **A506** 1 (1990).
- [25] L. Lapikas, G. van der Steenhoven, L. Frankfurt, M. Strikman and M. Zhalov, “The transparency of C-12 for protons,” Phys. Rev. C **61**, 064325 (2000).
- [26] H. Muether, Private communication; see also H. Muether, A. Polls, Prog. Part. Nucl. Phys. **45**, 243 (2000).
- [27] H. Feshbach, Theoretical Nuclear Physics, John Willey & Sons, 1990.
- [28] J. J. Cowan, F. -K. Thielemann, J. W. Truran, “The R-Processes and Nucleochronology,” Phys. Rep. **208**, 267-394 (1991).
- [29] L. Hoffman, A. Piepke, R. McKeown, B. Tipton, P. Vogel, “Background estimates for KamLAND from Natural Radioactivity of the Detector,” Internal report of KamLAND Collaboration, June 19, 2001, <http://citnp.caltech.edu/kamland/radioassay/rates/>; see also, F. Suekane (for KamLAND Collaboration), in *Proceedings of the Conference "Beyond the Desert 2002"*, Finland, Oulu, June 3-7, 2002.
- [30] E. Kolbe, “Untersuchungen zur inelastischen Neutrinostreuung an Kernen und Anwendungen in der Kern- und Astrophysik,” thesis, Universität Münster (1992).
- [31] K. Langanke, P. Vogel, E. Kolbe, “Signal for supernova  $\nu_\mu$  and  $\nu_\tau$  neutrinos in water Čerenkov detectors,” Phys. Rev. Lett. **76**, 2629 (1996).